Photochromic DTE-Substituted-1,3-di(2-pyridyl)benzene Platinum(II) Complexes: Photo-modulation of Luminescence and Second-order Nonlinear Optical Properties

Hong Zhao, Eleonora Garoni, Thierry Roisnel, Alessia Colombo, Claudia Dragonetti, Daniele Marinotto, Stefania Righetto, Dominique Roberto, Denis Jacquemin, Julien Boixel, et al.

Photochromic DTE-Substituted-1,3-di(2-pyridyl)benzene Platinum(II) Complexes: Photo-modulation of Luminescence and Second-order Nonlinear Optical Properties

Hong Zhao,[a] Eleonora Garoni,[b] Thierry Roisnel,[a] Alessia Colombo,[b,c] Claudia Dragonetti*,[b,c] Daniele Marinotto,[c] Stefania Righetto,[b] Dominique Roberto,[b,c] Denis Jacquemin*,[d] Julien Boixel*,[a] and Véronique Guerchais[a]

[a] Univ Rennes, CNRS, ISCR – UMR6226, F-35000, Rennes, France.
Email: julien.boixel@univ-rennes1.fr
[b] Dipartimento di Chimica, Università degli Studi di Milano and UdR INSTM di Milano, via Golgi 19, Milano, 20133, Italy.
Email: claudia.dragonetti@unimi.it
[c] ISTM-CNR, CIMAINA and SmartMatLab, via Golgi 19, Milano, 20133, Italy.
[d] Laboratoire CEISAM, UMR CNRS 6230, Université de Nantes, 2 rue de la houssinière, 44322 Nantes Cedex 03, France.
Email: denis.jacquemin@univ-nantes.fr
† Electronic Supplementary Information (SI) available:

Abstract: We disclose a new family of photochromic cyclometalated platinum(II) complexes (**PtDTE1** and **PtDTE2**), where a dithienylethene (DTE) unit is connected at the *para*-position of the central phenyl ring of (N^C^N) cyclometalated ligand, through two different linkages. Their syntheses are presented along with the X-ray characterizations of both the *open* and *closed* isomers of **PtDTE1**. The investigation of their photophysical properties is made, including absorption, photochromism, emission, and second-order nonlinear properties. We report a quantitative photo-isomerization for both **PtDTE1** and **PtDTE2**, irrespective of the nature of the connecting mode between the DTE unit and the platinum(II) moiety. The efficient photochromism allows a significant NLO photo-modulation, both in solution and in thin films. In addition, we show that the photoluminescence of the **PtDTE1** and **PtDTE2** can be controlled by the *open/closed* isomerization of the DTE unit.

Introduction

External control of intrinsic molecular properties fascinates scientists since decades, because of both fundamental challenges and practical concerns.[1] In particular, the modulation of the optical properties is of increasing interest for the development of new generations of functional molecular materials, notably in the fields of optical communication and data processing. Transition metal complexes attractively benefit from optical-active transitions tunable by the metal and the surrounding ligands which may pave the way to valuable luminescence and second-order nonlinear optical (NLO) properties.[2] Among the methods allowing to switch the linear and nonlinear optical responses of coordination compounds, the use of light is particularly fascinating since it can give rise to all-optical molecular systems, where light is able to write, store and read the information. Among photochromic compounds, dithienylethenes (DTE) generally show outstanding photochromic performances in terms of high photo-conversion, thermal stability and strongly contrasted optical signatures between the two isomeric *open (o)* and *closed (c)* forms.[3] Subsequently, DTE have been successfully employed as organic photo-switches in various fields such as photo-responsive optoelectronic and probes.[4] In view of these excellent photochromic abilities, investigations of structure/property relationships in DTE-based metal complexes have started recently, aiming to design more efficient systems.[5]

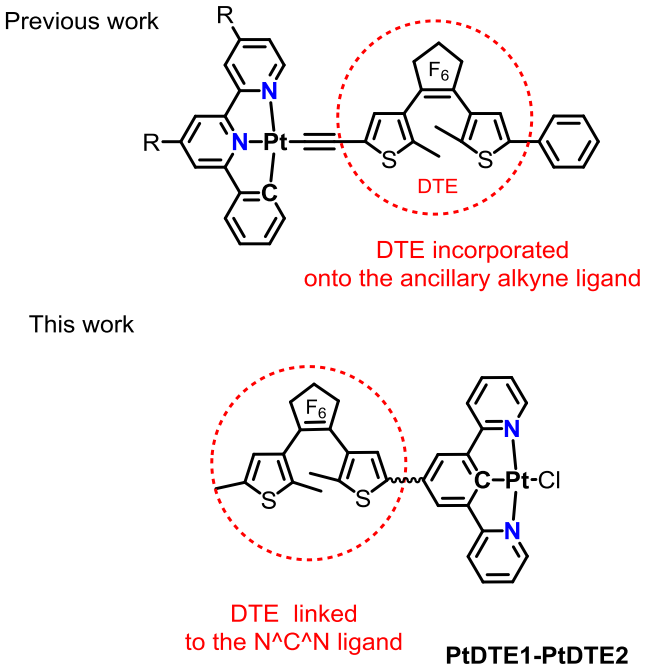

Chart 1. Structural representations of DTE-based (N^N^C)Pt-alkynyl (top) and (N^C^N)PtCl **PtDTE1(o)** and **PtDTE2(o)** (bottom).

In this context, our groups have been investigating cyclometalated (N^N^C)platinum(II) complexes (N^N^C = 4,4'-

di(*tert*-butyl)-6-phenyl-2,2'-bipyridine) bearing an alkynyl ligand functionalized with a DTE unit, with the aim of combining the optical properties of cyclometalated alkynylplatinum(II) complexes to the photochromic performances of DTE.[6] In these systems, the DTE is introduced on the ancillary ligand of the Pt(II) complex (Chart 1). Such approach allows an efficient photo-modulation of the NLO response of the complex during the photo-isomerization of the DTE, with an enhanced NLO signal for the closed form resulting from the extended π-conjugated length and the increased charge transfer character found in the closed isomer. We have indeed observed a remarkable photo-modulation of the NLO activity both in solution and thin films[6a] and a double sequential modulation of the NLO activity triggered by protonation and controlled by photochromism.[6b]

Cyclometalated (N^C^N-dpyb)platinum(II) complexes (dpyb = 1,3-di(2-pyridyl)benzene) constitutes another interesting family of NLO-active species.[7] For example, some of us reported that the functionalization of the N^C^N-pyridine rings with electron withdrawing groups (F, CF_3) greatly enhances the NLO response of the corresponding platinum complexes.[7a] Recently, the introduction of electron π-delocalized moieties on the *para*-position of the central benzene ring of the dpyb ligand was also found to constitute an efficient method for increasing the NLO response of these complexes. In particular, the introduction of a terthiophene produces large quadratic hyperpolarizabilities, as a result of the strong π-delocalization along a planar backbone.[7b]

These recent observations prompted us to investigate DTE-based (N^C^N)Pt(II) complexes where the DTE unit is linked on the *para*-position of the central benzene ring of the dpyb through one of the thiophene rings (Chart 1). Such design would lead to a photo-modulation of the π-delocalization system over the cyclometallated ligand, via open/closed isomerization of the pendant DTE, and consequently of the NLO response of the complex.

In addition, (N^C^N-dpyb)PtCl complexes are amongst the brightest emitters in solution at room temperature, partly due to a short Pt-C bond within the N^C^N coordination environment.[8] Therefore, this family of complexes has been used for OLEDs[9] and bio-imaging.[10] Interestingly, their luminescence which originates from a ligand-centered ^{3}LC state can be modulated by altering the electronic nature of the terdendate ligand. In particular, a judicious functionalization at the *para*-position of the central phenyl ring of the N^C^N ligand allows to tune the emission wavelength over the whole visible spectrum.[8] Thus, the presence of the DTE unit introduced onto the N^C^N ligand would offer the opportunity to also photo-control the luminescence of the complex.

In the present work, we report for first photo-modulation of both linear and nonlinear optical properties of two new DTE-based 1,3-dipyridylbenzene platinum(II) complexes, **PtDTE1** and **PtDTE2** (Figure 1). These two complexes differ by the linker separating the DTE unit and the (dpyb)PtCl fragment. The DTE moiety is directly connected to the central benzene ring of the terdentate ligand in **PtDTE1** whereas, in complex **PtDTE2**, it is separated by a non-conjugated and flexible ethylene glycol bridge. These different designs allow to understand the impact of the connecting mode and of the distance between the DTE unit and the (N^C^N)Pt(II) fragment on the photo-regulation of the optical properties. We present below the synthesis and full characterization of **PtDTE1, PtDTE2** and the free-DTE Pt(II) complex **Pt1** containing the 5-(5-methylthienyl)-1,3-di(2-pyridyl)benzene ligand, (Figure 1), used for comparisons.

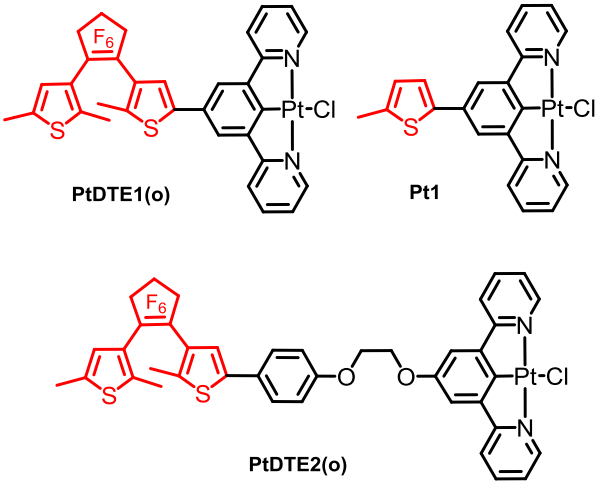

Figure 1. Chemical structures of the investigated *para*-substituted(1,3-dipyridylbenzene) PtCl complexes.

In addition, we describe herein the X-ray crystal structures of both *open* and *closed* forms of **PtDTE1,** no crystallographic studies of the two isomeric forms of a cyclometalated DTE-based platinum complex have been reported so far, to our knowledge.

Next, the absorption, photochromic and luminescence properties of all complexes have been investigated and rationalized with the aid of theoretical calculations. Moreover, the second-order NLO activity in solution has been studied for **Pt1, PtDTE1** and **PtDTE2** by means of the EFISH (Electric-Field Induced Second Harmonic Generation) technique[11] working with an incident wavelength of 1907 nm. Besides, due to the importance of second-order NLO active polymeric films for NLO applications,[5c] complex **PtDTE1** was dispersed and oriented by poling both in a polymethylmethacrylate (PMMA) and a polystyrene (PS) matrix affording composite films from which Second Harmonic Generation (SHG) is investigated. The experimental results are accompanied by theoretical calculations as well in order to get a better understanding of the parameters that govern the second-order NLO photo-modulation in this kind of complexes.

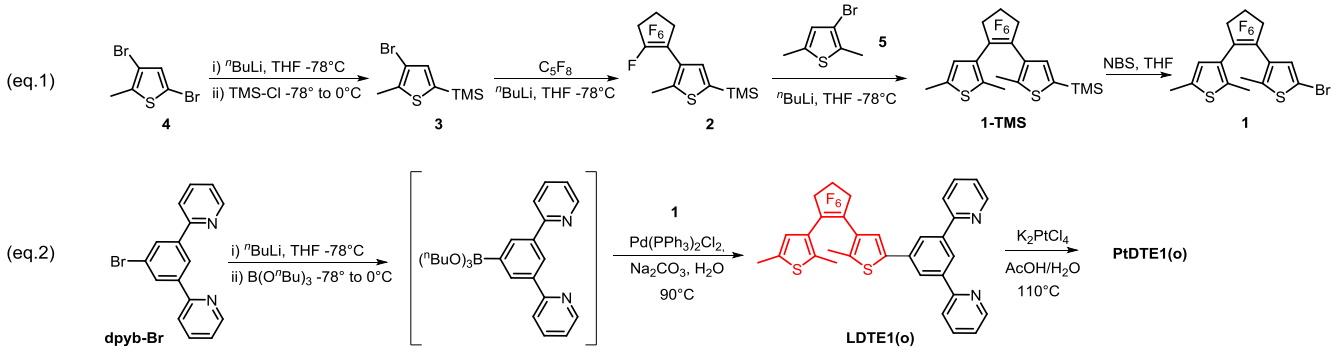

Scheme 1. Synthesis of **LDTE1(o)** and **PtDTE1(o)**

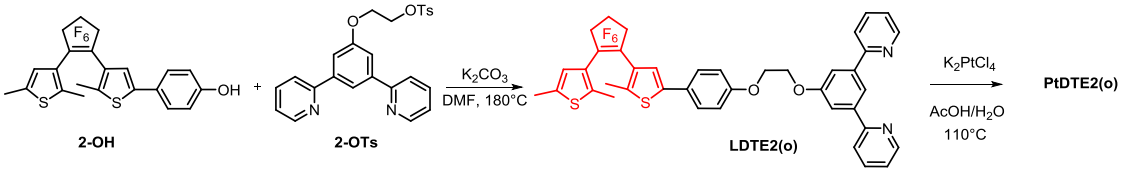

Scheme 2. Synthesis of **LDTE2(o)** and **PtDTE2(o)**

Results and Discussion

Synthesis of ligands and complexes. Schemes 1 and 2 show the synthesis of the target DTE-based Pt(II) complexes **PtDTE1** and **PtDTE2** and that of the corresponding ligands **LDTE1-2**. The precursor ligand **LDTE1** has been prepared following a modified procedure of 5-aryl-susbtituted-1,3-dipyridylbenzene derivatives, where the introduction of the aryl substituent proceeds via a Suzuki cross-coupling reaction between 1-bromo-3,5-dipyridylbenzene (dpyb-Br) and the appropriate aryl boronic derivative.[8b] In the present case, the aryl precursor, namely DTE-based compound **1**, was obtained in six steps with an overall yield of 20 %, by sequential coupling the two thiophene moieties to the perfluorocyclopentene ring (Scheme 1, eq. 1). The terdentate ligand **LDTE1** was synthesized following eq. 2 (Scheme 1), dpyb-Br was first converted into its boronic derivative and subsequently treated with the bromo-DTE **1** to give **LDTE1** in good yield (67 %). The pro-ligand **L1**, of the complex **Pt1**, was obtained by coupling dpyb-Br with the 2-bromo-5-methylthiophene in similar conditions used for the synthesis of **LDTE1**.

LDTE2 was prepared by treatment of the phenol-DTE **2-OH**[12b] on the pro-ligand **2-OTs**,[13] bearing the ethylene glycol chain substituted by a tosylate (Scheme 2). Then, complexes **PtDTE1, PtDTE2** and **Pt1**, are readily obtained by treatment of the appropriate pro-ligand with potassium tetrachloroplatinate in an acetic acid – water (3 – 1, v/v) mixture at reflux.[8b] All complexes have been isolated in pure form by a simple filtration thanks to their low solubility in a AcOH/H_2O mixture. The ligands **LDTE1, LDTE2**, **L1** and complexes **PtDTE1, PtDTE2**, **Pt1** have been fully characterized by means of ^{1}H and ^{13}C NMR (Figures S1-S17 in SI), elemental analysis and mass spectroscopies. For ligands and complexes bearing the DTE photochromic unit, their open and closed forms are denoted as **(o)** and **(c)**, respectively, in the following. **PtDTE1** and **PtDTE2** have been isolated in their open forms and the ^{1}H NMR spectra of **PtDTE1(o)** and **PtDTE2(o)** exhibit the characteristic singlets for the two methyl substituents of the DTE unit, they are located at 1.92, 1.96 ppm and 1.88, 1.92 ppm, respectively (see experimental part and SI). In agreement with the spectroscopic data reported for thienyl-(N^C^N)Pt(II)Cl complex, the ^{1}H NMR signals of **Pt1** appear between 7.3 - 9.3 ppm which are assigned to the aromatic protons of the N^C^N ligand.[8b]

Table 1. Selected bond lengths [Å], angles [°] and torsion angle [°] for **PtDTE1(o)** and **PtDTE1(c)**.

PtDTE1(o)			
Bond length [Å]		Angles [°]	
Pt1-C7	1.903(5)	N2-Pt1-N1	161.01(18)
Pt1-N1	2.028(5)	C7-Pt1-N1	80.70(2)
Pt1-N2	2.037(4)	C7-Pt1-N2	80.36(19)
C17-C18	1.360(8)		
C18-C19	1.430(7)	Torsion angle [°]	
C20-C24	1.360(8)	C15-C16-C17-C18	37.10(9)
S1-C17	1.741(6)		
S1-C31	1.731 (6)		
PtDTE1(c)			
Bond length [Å]		Angles [°]	
Pt1-C7	1.913(10)	N2-Pt1-N1	161.00(18)
Pt1-N1	2.017(9)	C7-Pt1-N1	79.90(4)
Pt1-N2	2.036(8)	C7-Pt1-N2	81.20(4)
C17-C18	1.350(15)		
C18-C19	1.399(10)	Torsion angle [°]	
C20-C24	1.413(17)	C15-C16-C17-C18	-6.72(2)
C31-C29	1.400 (5)		
S1-C17	1.741(6)		
S1-C31	1.731 (6)		

Crystal structures. Single crystals of **PtDTE1(o)** and **PtDTE1(c)** (Figure 2, Tables S1 and S2) suitable for X-ray diffraction analysis were grown at room temperature by slow diffusion of diethyl ether vapor into concentrated dichloromethane solution of **PtDTE1** in its open and photostationary state (PSS). Selected bond lengths and angles of **PtDTE1(o)** are given in Table 1.

Complex **PtDTE1(o)** crystallizes in the P-1 space group (Figure 2, top). The platinum center displays a typical distorted square-planar geometry with an N-Pt-N angle of 161.01° and N-Pt-C angles of around 80°. The open DTE moiety adopts the anti-parallel configuration with a C29…C31 through space distance of 3.569 Å, suitable for photo-triggered ring-closure reaction.[14] The bond lengths of the DTE core follow expectations, with C17–C18 and C18–C19 distances of 1.360 and 1.430 Å, respectively, characteristics of carbon–carbon double and single bond of a thiophene ring. A large torsion angle of 37.10° is observed between the thiophene and the central phenyl ring (C15-C16-C17-C18) of the complex. This value is comparable to that observed for the related phenyl substituted-(N^C^N) platinum(II) complex (torsion angle 29.63°).[8b] By contrast, the angle for the metal-free 2-phenyl-substituted DTE(o) is three times smaller (10 – 20°),[14] this reflects the impact of the complexation of DTE to the platinum center via the N^C^N ligand.

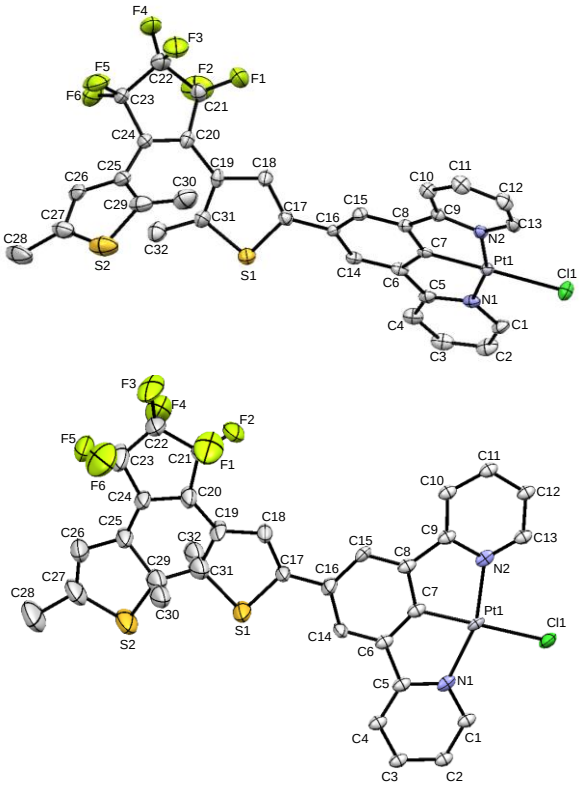

Figure 2. The perspective views of PtDTE1(o) (top) and of PtDTE1(c) (bottom). Thermal ellipsoids are shown at the 50 % probability level.

PtDTE1(c) crystallizes in the same P-1 space group as its open form (Figure 2, bottom). The structure shows that photo-isomerization of the DTE unit does not significantly affect the geometry at the metal center displaying a distorted square-planar geometry (Table 1). The major change in the structure is the new created single bond between C29 and C31. Because of free motions on the closed DTE part of the X-ray crystallographic analysis, the C29-C31 bond distance listed in Table 1 is very small (1.400 Å) and can be consequently considered as irrelevant. The DFT calculations predict C29-C31 distance of about 1.54 Å in perfect agreement with the previously reported XRD bond distances of closed DTE.[14] This value is probably more relevant than the one obtained from XRD. We consider this computed value as more realistic. Nevertheless, the XRD analysis clearly shows that a DTE photochrome in its closed form and we underline that X-Ray structures of *closed* dithienylethenes are rare.[14] To the best of our knowledge, this is the first example of a crystallographic structure for a closed cyclometalated DTE-based platinum complex.[15]

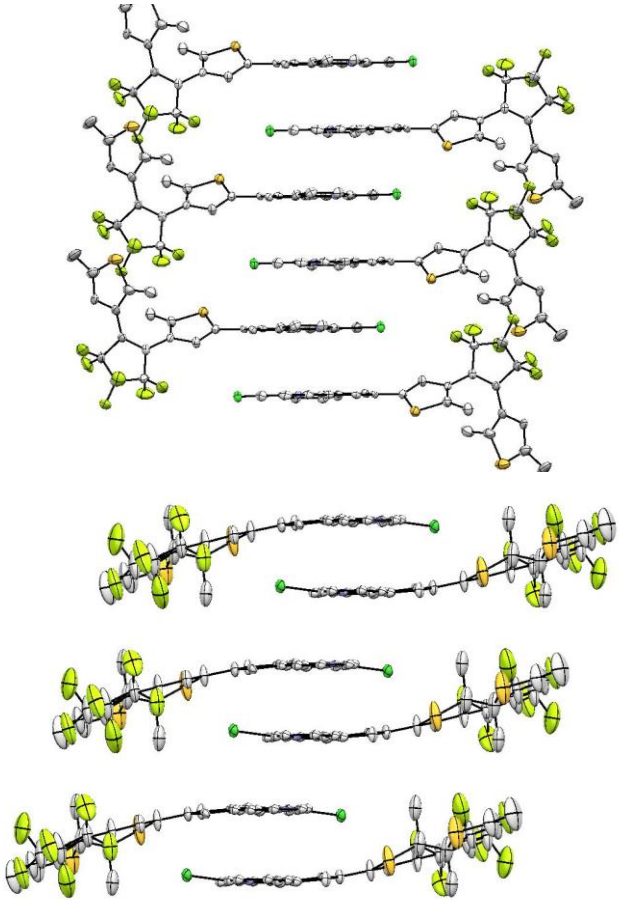

Figure 3. Representations of the packing for the **PtDTE1(o)** (*top*) and **PtDTE1(c)** (*bottom*) structures.

As a consequence of the rearrangement of the π-system upon ring-closure, the bonds between C17–C18 (1.350 Å) and C18–C19 (1.399 Å) have single and double bond characters, respectively, which is as expected. Additionally, the torsion angle between the thienyl of the DTE core and the phenyl group of the cyclometalated ligand becomes smaller (C15-C16-C17-C18 = 6.7°) with an evident bending of the molecule, suggesting an efficient π-delocalization over the complex. Such planarization in the cyclized DTE derivative with the adjacent phenyl rings was previously observed solely in the case of organic dithenylethenes.[14] Analysis of the crystal packing for **PtDTE1(o)** and **PtDTE1(c)**, presented in Figure 3, reveals a comparable offset head-to-tail arrangement, despite the different torsion angles between the DTE and the N^C^N fragment. Both structures consist of infinite stacks of molecules along a columnar arrangement of cyclometalated Pt centers, built with Pt-π and π-π interactions. It has been reported that small anisotropic shape changes occur from the *open* to the *closed*

forms in organic DTE.[3b] Consequently, in the present systems similar packing distances are observed between the *open* and the *closed* isomers, alternating between 3.448 and 3.365 Å for **PtDTE1(o)** and 3.227 and 3.263 Å for **PtDTE1(c)**, respectively.

Electronic absorption. The steady-state absorption spectra of the complexes **Pt1, PtDTE1(o)** and **PtDTE2(o)** recorded in dichloromethane solution are presented in Figure 4a while those of the ligands **LDTE1** and **LDTE2** are shown in Figure S18. The related data are summarized in Table 2. The electronic absorption spectra of **LDTE1** and **LDTE2**, in their open forms, exhibit solely transitions in the UV region, originating from π-π* transitions. **Pt1** shows absorption features similar to those reported for the 5-thienyl-1,3-dipyridylbenzene platinum(II) chloride complex (CH_2Cl_2) with intense absorption bands in the UV region, from 270 to 350 nm ($\varepsilon = 3.3\ 10^5\ M^{-1}cm^{-1}$) assigned to ligand centered (LC) $^1(\pi\text{-}\pi^*)$ transitions of the N^C^N ligand.[8b] The weaker absorption bands in the visible part of the spectrum, from 400 to 480 nm, are attributed with the help of theoretical modeling (*vide infra*), to charge transfer (CT) transitions from the thienyl, the metal and the chloride to the pyridine moieties of the N^C^N ligand.

Table 2. UV-visible absorption data of the investigated platinum complexes.

	λ_{abs}[a]/nm (ε $10^{-4}/M^{-1}cm^{-1}$) Open ***(o)*** forms	λ_{abs}[a,b]/nm Closed ***(c)*** forms (PSS)
LDTE1	305 (50.5), 355 (4.27)	303, 360, 560
LDTE2	280 (45.7), 310 (23.4)	278, 314, 354, 552
PtDTE1	300 (48.8), 382 (5.9), 418 (6.7), 432 (6.6)	293, 335, 352, 368, 410, 567
PtDTE2	296 (40.8), 379 (6.0), 420 (6.4), 437 (6.5)	296, 328, 370, 418, 439, 551
Pt1	303 (33.3), 382 (4.6), 420 (5.4), 437 (5.3)	

[a] Measured in CH_2Cl_2 solution at 298 K. [b] After irradiation at 350 nm.

The absorption profiles of the open DTE-based Pt(II) complexes **PtDTE1(o)** and **PtDTE2(o)** are similar to that of **Pt1** (Figure 4a). The presence of the DTE moiety in **PtDTE1(o)** and **PtDTE2(o)** can be seen in the UV region with an enhanced absorptivity, due to additional $^1(\pi\text{-}\pi^*)$ transitions centered on the DTE. For **PtDTE1(o)**, in the visible part of the spectrum the lowest-energy absorption bands are slightly blue-shifted (5 nm) compared to **Pt1**, probably due to the electron-withdrawing properties of the perfluorocyclopentene moiety, directly connected to the thiophene substituent. The absorption spectral features of **PtDTE2(o)** are comparable to those of the reported 4-methoxy-subtituted-(N^C^N)platinum(II) chloride complex.[8e] These similar absorption profiles between the DTE-based complexes **PtDTE1(o)** and **PtDTE2(o)** and the reference compound **Pt1**, particularly in the CT region, indicate that the ground-state electronic absorption properties of the cyclometalated Pt(II) are not strongly affected by the presence of the adjacent open DTE. This is also consistent with the orbital topologies (*vide infra*).

Photochromism. Interconversions between the open and closed forms of **LDTE1**, **LDTE2**, **PtDTE1** (Scheme 3) and **PtDTE2** have been monitored by UV-visible absorption in CH_2Cl_2 (Figure 4 and S18) and proton NMR spectroscopy (Figure 5, Figure S8, S11 and S17). 350 and 580 nm light irradiations are used to trigger the cyclization and the

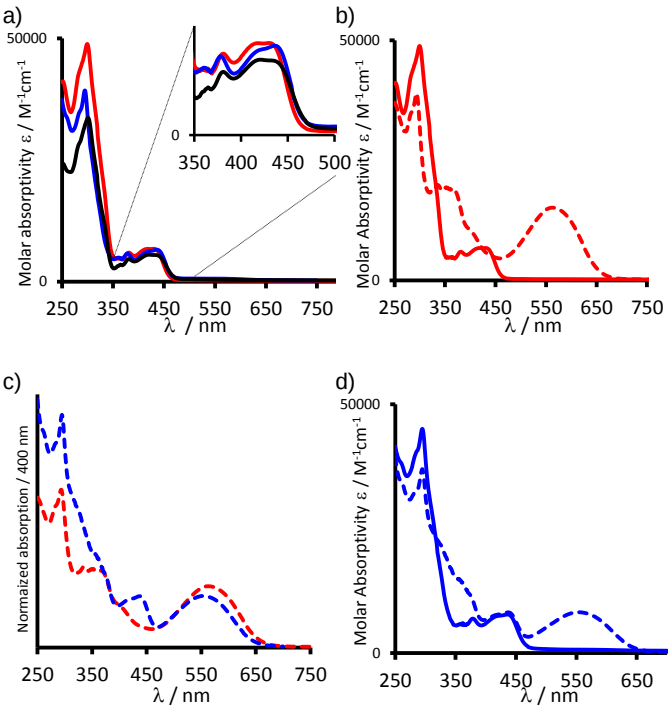

Figure 4. Absorption spectra in CH_2Cl_2 at 298 K ($C \approx 10^{-5}$ M) of a) **Pt1** (black line), **PtDTE1(o)** (red line) and **PtDTE2(o)** (blue line). b) **PtDTE1**, before (plain) and after (dashed) irradiation at 350 nm c) Normalized absorption spectra at 400 nm of **PtDTE1(c)** (red), **PtDTE2(c)** (blue), in their *closed* (PSS) forms. d) **PtDTE2**, before (plain) and after (dashed) irradiation at 350 nm.

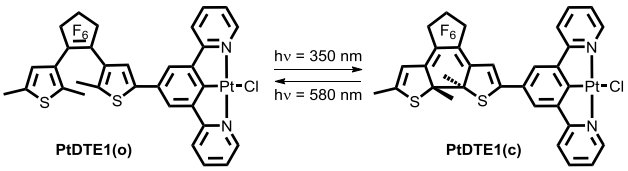

Scheme 3. Photochromic reaction of complex **PtDTE1**.

cycloreversion reactions, respectively (Scheme 3). The initial pale yellow solution of **PtDTE1(o)** turns dark blue upon irradiation at 350 nm with the emergence of a large absorption band in the visible, centered at 567 nm, attributed to $^1(\pi\text{-}\pi^*)$ transition on the closed DTE unit of **PtDTE1(c)** (Figure 4b).[3] Irradiation of **PtDTE1(c)** at 580 nm quantitatively yields back the open form **PtDTE1(o)**, showing the good reversibility of this system.

It can be seen in Figure 4b that the absorption bands (λ_{abs} around 350 – 450 nm) of **PtDTE1(o),** attributed to CT transitions, are modified upon ring-closure reaction. This feature is consistent with the presence of an electronic communication between the (N^C^N)Pt fragment and the closed DTE unit, which is also supported by the shape of the corresponding LUMO that is delocalized (see SI). Also, the maximum in absorption of the broad visible band in **PtDTE1(c)** is slightly red-shifted of about 7 nm in comparison with **LDTE1(c)** (Figure S18 and Table 2). **PtDTE2(o)** also exhibits excellent photochromic properties upon UV irradiation. The hallmark absorption band of the closed DTE appears at 551 nm, i.e., is blue-shifted by ca. 16 nm compared to **PtDTE1(c)** (Figure 4c) due to the absence of

electronic delocalization with the (N^C^N) ligand and the presence of the electron donating ethylene glycol bridge. Besides, this lower-energy absorption band at 551 nm for **PtDTE2(c)** is comparable to the one of the ligand **LDTE2** (550 nm, Figure S18) and to that reported for organic DTE substituted by an anisole group.[12] As expected with the presence of the saturated ethylene glycol linkage between the Pt(II) and the DTE moieties, the CT transitions of the (N^C^N)Pt(II) fragment (from 400 to 480 nm) are unaffected by the photoisomerization (Figure 4d). As for complex **PtDTE1**, the open form **PtDTE2(o)** is fully recovered upon irradiation at 580 nm. Comparing the photochromic properties of complexes **PtDTE1** and **PtDTE2** (Figures 4 and S19), one can say that the presence of the Pt(II) fragment directly coupled or not to the DTE core, displays roughly a similar rate of conversion upon UV irradiation.[16a] By contrast, upon visible irradiation, the presence of a saturated linker induces a lower rate of photocyclization.[16]

Monitoring the ring-closure reaction by ^{1}H NMR spectroscopy gives access to the percentage of conversion at the photostationary state (PSS). Figure 5 shows the ^{1}H NMR spectra of **PtDTE1** before and after irradiation at 350 nm. The characteristic ^{1}H NMR spectral changes are observed,[6a] with upfield shifted singlets (from 7.36 to 6.80 ppm and from 6.77 to 6.06 ppm) assigned to the thienyl protons of the DTE core, together with downfield shifted singlets (from 1.92 and 1.96 to 2.14 and 2.16 ppm) corresponding to the methyl protons. The relative integration of the above methyl signals between the open and the closed form of **PtDTE1** shows an almost quantitative photo-conversion with a PSS as high as 95 %.

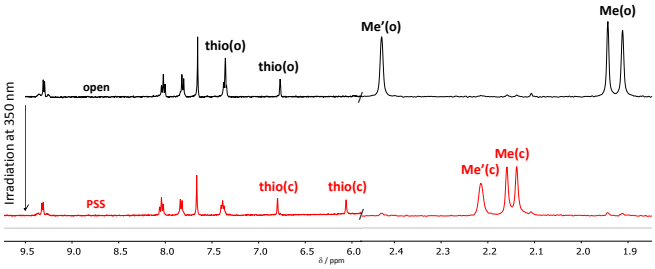

Figure 5. Partial ^{1}HNMR spectra of **PtDTE1** in CD_2Cl_2, before (black) and after (red) irradiation at 350 nm.

Interestingly, the photochromic reaction of **PtDTE2** investigated by proton NMR spectroscopy also reveals an almost quantitative open to closed photo-conversion (> 95%, Figure S17). In contrast, the conversion of the free ligands **LDTE1** and **LDTE2** is lower than that of the corresponding complexes upon UV irradiation. Indeed, the rate of photoisomerization to the closed form, determined from by ^{1}H NMR spectroscopy, is 50 and 30% for **LDTE1** and **LDTE2**, respectively (See Figures S8 and S11). The beneficial effect of the Pt ion coordination on the photochromic properties has never been reported previously, to our knowledge.[17] As shown by ^{1}H NMR studies (Figures S8 and S11), UV irradiation of the free-ligands **LDTE1** and **LDTE2** leads to some partial decomposition while under the same conditions, the presence of the coordinated Pt(II) ion, in **PtDTE1** and **PtDTE2**, prevents the formation of any side products. These experimental results illustrate the beneficial role of the complexation in the present cases.

Notably, upon irradiation into the visible (at 450 nm), namely in the CT absorption bands, both **PtDTE1** and **PtDTE2** show conversions as high as when using 350 nm excitation (Figure S14) although a markedly slower rate of photo-cyclisation is monitored for **PtDTE2** upon 450 nm light excitation (see Figure S19). This behavior, reported as a DTE ring-closure sensitization, was previously demonstrated for DTE-based Pt(terpyridine)(alkynyl) complexes where the DTE is connected to the alkynyl ligand and explained as an intra-molecular triplet energy transfer from the ^{3}CT states of the complex to the ^{3}IL (Intra-Ligand) state localized on the open DTE.[16] In particular, a former study demonstrated that reducing the orbital overlap between the metal-based and open DTE states, by breaking the conjugated pathway, dramatically diminishes the efficiency of the metal-sensitized photocyclization reaction.[16b] Curiously, in the present designs of **PtDTE1** and **PtDTE2**, the efficiency of the energy transfer toward the photoactive $^3IL_{DTE}$ appears to be quantitative irrespective of the nature of the linkage, though, as mentioned above the reaction rate is slower in **PtDTE2**. For **PtDTE1** the efficiency can be rationalized by the delocalization of the spin density of the triplet excited state over the DTE, see the theoretical calculations (*vide infra*). In **PtDTE2** the efficient ring-closure sensitization may be attributed to the possible proximity between the (N^C^N)PtCl and DTE fragments, thanks to the flexible ethylene glycol linkage, such proximity allowing for efficient through-space energy transfer. In this framework, we underline that the selected linker has been shown to be too short to allow significant overlap between the electron densities of the two fragments, so that such direct interaction is unlikely to explain the observed sensitization.[18]

Photoluminescence of complexes. Room temperature emission measurements of **Pt1, PtDTE1 and PtDTE2.** were performed in degassed dichloromethane solution with a concentration of ca. 10^{-6} M, diluted enough so that excimer emission can be excluded (Figure 6a).[8a] The luminescence at 77K in EPA matrix (diethyl ether/isopentane/ethanol: 2/2/1) was also investigated for all complexes (Figure 6b). The photoluminescence data are collected in Table 3.

Pt1 exhibits similar photoluminescence characteristics, in dichloromethane solution at 298 K, as those reported for the (5-thienyl-substituted-dpyb)PtCl complex[8b], with an intense emission in the green region of the spectrum (0-0 emission band at λ = 558 nm). The emission band of **Pt1** is structured (vibrational spacing of about 1300 cm^{-1}) and the lifetime is in the microsecond time range; signatures that are typical of a ligand centered (LC) triplet emission character. Also, the photoluminescence quantum yield (28 %) compares well with those of analogue complexes.[8]

Table 3. Emission data of the investigated platinum complexes.

	Emission at 298 K[a]		Emission at 77 K[c]
	λ_{em}/nm (τ/μs)	Φ_{em}[b]	λ_{em}/nm (τ/µs)
PtDTE1	547 (*6.1*), 588, 655sh	-	538 (*23.5*), 584, 638
PtDTE2	545 (*7.0*), 578	-	532 (*13.3*), 576, 623
Pt1	558 (*9.2*), 600, 655 sh	0.28	547, 593, 653

[a] Measured in degassed CH_2Cl_2 solution at 298 K (C ≈ 10^{-5} M), with 440 nm light excitation. [b] ref: $Ru(bpy)_3Cl_2$. [c] in EPA (ethanol/isopentane/diethylether : 2/2/1) glass at 77 K, λ_{ex} = 440 nm.

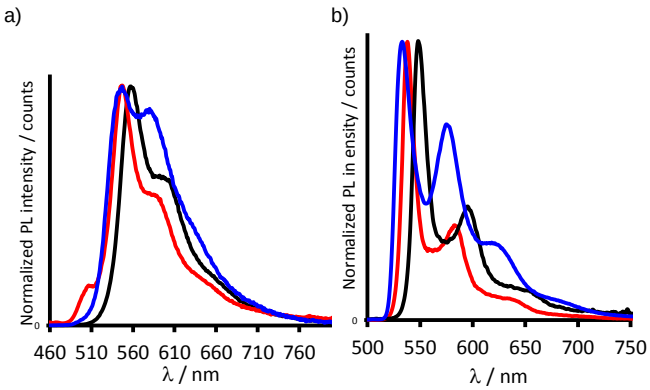

Figure 6. Emission spectra of complexes **Pt1** (black), **PtDTE1(o)** (red) and **PtDTE2(o)** (blue) in, a) degassed CH_2Cl_2 at 298 K and b) EPA (diethyl ether/isopentane/ethanol: 2/2/1) glass at 77 K, λ_{ex} = 440 nm.

The emission spectrum of the DTE-based complex **PtDTE1(o)** (Figure 6a) exhibits a similar spectral profile as that of **Pt1** with an hypsochromic shift (11 nm) of the whole spectrum, attributed to the presence of the electron-withdrawing perfluorocyclopentene moiety. However, the photoluminescence quantum yield (Φ < 1 %) is very weak, probably due to a competitive ring-closure reaction occurring through metal-sensitized pathway in its open form. This is also supported by the appearance of a blue coloration of the solution after the emission measurement upon photo-excitation at 440 nm, an irradiation wavelength which can efficiently trigger the ring-closing process, especially in very dilute conditions.[16] To confirm this proposal, we performed emission studies of **PtDTE1** at the *PSS* (Figure S20). This leads to the same result, with a quantum yield Φ less than 1 % and a luminescence spectrum similar to that obtained by starting with **PtDTE1(o)**. This indicates that an efficient sensitized ring-closure occurs during the photoluminescence measurements. The emission spectra observed in both cases can be attributed to the remaining open isomer **PtDTE1(o)**.

Notably, **PtDTE2(o)** exhibits the same behavior as **PtDTE1(o),** and the weak emission observed for **PtDTE2(o)** is attributed to the remaining open isomer **PtDTE2(o**). The spectrum displays a characteristic structured emission band comparable to those reported by de Cola for the related DTE-free Pt(II) complexes bearing a N^C^N cyclometalated 1,3-di(2-pyridyl)-benzene ligand substituted with an ethylene glycol moiety.[13] From these findings, we deduce that the linker separating the DTE unit and the terdentate ligand does not significantly impact the quenching of the luminescence. This contrasts with the behavior of the related DTE-based terpyridine Pt(II)-acetylide, in which the presence of an ether linkage between the DTE and the Pt(II) fragments diminishes the rate of the metal-sensitized ring-closure reaction and changes the luminescent properties significantly.[16] One can assume that the flexibility and the length of the linker in **PtDTE2** may allow to bring the DTE and the (N^C^N)PtCl moieties sufficiently close to promote through-space energy transfers and facilitate the luminescence quenching.

Figure 6b shows the luminescence spectra of **Pt1**, **PtDTE1(o)**, and **PtDTE2(o)** recorded in EPA at 77 K. The emission spectrum of **Pt1** exhibits highly structured vibronic bands. The highest energy emission band is blue-shifted by ca. 11 nm compared to the 298 K emission. At 77 K, we assume that the competitive ring-closure reaction of the DTE is suppressed,[7] and consequently the observed emission band can be attributed to the *fully* open form of **PtDTE1** and **PtDTE2**. Their emission spectra are similar to that of **Pt1** with a blue-shift (9 and 15 nm, respectively), compared to the solution spectra. The 77 K emission features of **PtDTE2** compare well with those reported for (5-methoxy-1,3-dpyb)PtCl.[8e]

To probe the influence of the linker in **PtDTE1** and **PtDTE2** on the metal-sensitized DTE ring-closure, variable temperature emission measurements were conducted upon irradiation with 440 nm light, in an EtOH/MeOH (4/1) mixture (Figure 7). The photocyclization process depends on the viscosity of the medium, a rigid matrix inhibits any motion needed for the ring-closure reaction. But more importantly, as previously reported the metal-sensitized DTE ring-closure process, from the ^{3}CT to the $^3IL_{DTE}$ state, requires sufficient thermal energy to overcome the barrier between those triplet states.[16] Emission spectra were recorded from 85 K to room temperature with 10 K steps. For **PtDTE1**, the emission spectrum measured at 85 K resembles the one recorded in EPA at 77 K (Figure 7b), telling us that the metal-sensitized DTE ring-closure process is inhibited at this temperature. Increasing the temperature of the **PtDTE1** solution progressively triggers the metal-sensitized DTE ring-closure process, which competes with the luminescence. For **PtDTE1** the luminescence intensity starts to decrease from around 95 K and a complete luminescence quenching is recorded at 155 K (Figure 7a).[7b] Similarly, for **PtDTE2**, the well-structured luminescence spectrum at 85 K becomes less intense as the temperature increases with total luminescence quenching at 250 K (Figure 7b). The requirement of a higher temperature for a complete luminescence quenching in **PtDTE2**, versus **PtDTE1**, clearly hints at a less efficient energy transfer that we relate to the flexibility, nature and length of the linker between the DTE and (N^C^N)PtCl moieties.

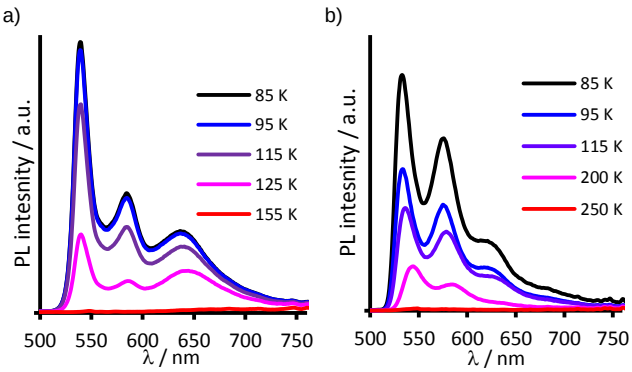

Figure 7. Emission spectra in degassed EtOH/MeOH : 4/1 mixture of a) **PtDTE1**, b) **PtDTE2** at variable temperatures from 85 to 250 K. λ_{ex} = 440 nm.

It is interesting to point out that with the above conditions a complete quenching of luminescence is observed for both complexes, indicating that there is no remaining *open* form. This result contrasts with the observations at room-temperature where residual emission is due to the presence of a small share open isomer at the photo-stationary state (PSS) in both cases.

The temperature was shown to affect the height of the thermal activation barriers of DTEs, leading to a decrease of the ring-opening process when lowering the temperature while the ring-closure reaction remains almost unaffected.[16,19] Consequently, this feature can be explained by the inhibition of the ring-opening reaction at temperature below 130 K whilst the photocyclization still occurs, leading to an accumulation of the closed isomer up to the full conversion.

Second-order nonlinear optical properties. The second-order NLO properties in solution of complexes **Pt1**, **PtDTE1(o)** and **PtDTE2(o)** were investigated by the EFISH technique that provides direct information on the intrinsic molecular NLO properties through,[11]

$$\gamma_{EFISH} = (\mu\beta_{EFISH}/5kT) + \gamma(-2\omega; \omega, \omega, 0) \quad (1)$$

where $\mu\beta_{EFISH}$ /5kT is the dipolar orientational contribution and $\gamma(-2\omega; \omega, \omega, 0)$, a third order term at frequency ω of the incident light, is a purely electronic cubic contribution to γ_{EFISH} which can usually be neglected when studying the second-order NLO properties of dipolar compounds.[2]

In Table 4 we report the $\mu\beta_{1.907\ EFISH}$ values for all the investigated complexes, measured in CH_2Cl_2 solution with an incident wavelength of 1.907 μm. To obtain $\beta_{1.907\ EFISH}$, the projection along the dipole moment axis of the vectorial component of the tensor of the quadratic hyperpolarizability, it is necessary to know the dipole moment, μ. In the present study we used theoretically determined dipole moments.

Table 4. $\mu\beta_{1.907\ EFISH}$, μ and $\beta_{1.907\ EFISH}$ of the investigated Pt(II) complexes.

Complex	$\mu\beta_{1.907\ EFISH}$[a] ($x10^{-48}$ esu)	μ[b] (D)	$\beta_{1.907\ EFISH}$ ($x10^{-30}$ esu)
Pt1	-516	8.9	- 58
PtDTE1(o)	-510	8.9	- 57
PtDTE1(c)	-1450	7.1	- 204
PtDTE2(o)	-575	15.4	- 37
PtDTE2(c)	-1476	8.9	- 166

[a] Working in CH_2Cl_2 with an incident radiation wavelength of 1.907 μm; the error is 10%. [b] Calculated at the DFT level in CH_2Cl_2 (see Experimental Section).

In agreement with other cyclometalated (N^C^N-dpyb)platinum(II)compounds,[7] all the investigated complexes are characterized by a negative value of $\mu\beta_{1.907\ EFISH}$, irrespective of the form of the DTE unit (open or closed), as expected for a negative value of $\Delta\mu_{eg}$ (difference of the dipole moment in the excited and ground states) upon excitation.[2] In these complexes, the decrease of the dipole moment upon excitation is consistent with a second-order dipolar NLO response dominated by the charge transfer from platinum to the cyclometallated ligand.[7] Similar and rather large values are obtained for **Pt1** and **PtDTE1(o)** indicating that the substitution of the methyl substituent by the perfluorocyclopentene moiety does not significantly affect the second-order NLO response. Upon irradiation at 350 nm of the solution of **PtDTE1(o)**, a three-fold increase of the $\mu\beta_{1.907\ EFISH}$ is observed due to the closure of the DTE unit (PSS). This large enhancement of the quadratic NLO response upon ring-closing is attributed to the augmented delocalization of the π-conjugation in the closed form, accompanied by an important decrease of the HOMO-LUMO gap, leading to a four-fold increase of the quadratic hyperpolarizability which more than compensates for the small decrease of the dipole moment (Table 4). Similarly, an increase of the second-order NLO response was previously observed upon ring-closure of DTE-based (N^N^C)Pt acetylide complexes ($\mu\beta_{1.907\ EFISH}$ = -180 and -1150×10^{-48} esu for the open and closed forms, respectively) that, however, were characterized by much lower luminescence efficiencies[6] (Chart 1).

For **PtDTE2**, it turns out that the open form of the complex is characterized by a lower quadratic hyperpolarizability than in both **Pt1** and **PtDTE1** but by a higher dipole moment leading to similar $\mu\beta_{1.907\ EFISH}$ values. Surprisingly, although the DTE moiety is separated from the N^C^N fragment in complex **PtDTE2(o)**, the $\beta_{1.907\ EFISH}$ value increases upon ring-closing to form **PtDTE2(c)**, with an enhancement factor similar to that observed on going from the open to the closed form of **PtDTE1** where the DTE moiety is directly connected to the N^C^N fragment. This unexpected NLO behavior of **PtDTE2** represents, to the best of our knowledge, the first example where closure of a DTE moiety not π-conjugated to the coordination sphere significantly influences the quadratic hyperpolarizability of a metal complex.

To study the second-order NLO properties of **PtDTE1** in the solid state, thin films of the chromophore dispersed in a polymethylmethacrylate (PMMA, Figure S21) or polystyrene (PS) matrix, as reported in the experimental section have been prepared. It turns out that the SHG signal of films in PMMA progressively fades due to a loss of orientation of the dyes (Figures S22 and S23).

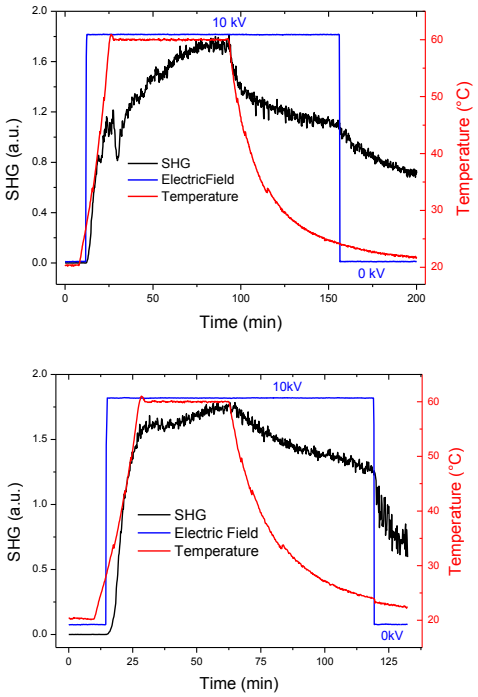

Figure 8. Poling of the **PtDTE1/**PS films in the closed (*top*) and open (*bottom*) forms.

This behavior, already reported in some previous works,[20] is not surprising if the β transition of PMMA, which has been attributed to rotation of the ester side group,[21] is considered. A much more valuable behavior is obtained by using polystyrene as matrix. Thus, poling is made on polystyrene films of complex **PtDTE1** either in the open or closed forms (Figure 8). The SHG response is negligible before applying the corona voltage but it quickly increases after application of the electric field. When the temperature is increased up to 50-60°C, a large increase of the SHG occurs, due to the decrease of the viscosity of the polymeric matrix which allows an easier orientation of the NLO chromophores. When a stable SHG signal is reached, the sample is cooled at room temperature, the final switch off of the electric field inducing some drop of the SHG.

After poling, both the open and the closed forms of the **PtDTE1**/PS film show a slight decrease of absorption peaks in comparison with that observed before poling (Figure S24); this is the characteristic so-called dichroic effect due to the partial orientation of molecules along the direction of the electric poling field (*Z* axis).[6] No appreciable Stark shift[22] of the absorption peaks was observed after poling.

By fitting the Maker fringe measurements,[23] the three nonzero coefficients of the second-order susceptibility tensor $\chi_{33}^{(2)}$, $\chi_{31}^{(2)}$ and $\chi_{15}^{(2)}$ for a poled film have been evaluated (Table 5).

Table 5. Second-order susceptibility tensor of **PtDTE1/**PS films in open and closed forms.

Complex	$\chi_{33}^{(2)}\ (pm/V)$	$\chi_{31}^{(2)}\ (pm/V)$	$\chi_{15}^{(2)}\ (pm/V)$	$\chi_{33}^{(2)}/\chi_{31}^{(2)}$	$\chi_{33}^{(2)}/\chi_{15}^{(2)}$
PtDTE1(o)	0.56	0.58	0.15	0.96	3.73
PtDTE1(c)	2.82	1.74	0.54	1.62	5.22

As shown in Table 5, for **PtDTE1/**PS films the $\chi_{33}^{(2)}$, $\chi_{31}^{(2)}$ and $\chi_{15}^{(2)}$ values increase going from the open to the closed form. Besides, the ratios of the components $\chi_{33}^{(2)}/\chi_{31}^{(2)}$ and $\chi_{33}^{(2)}/\chi_{15}^{(2)}$ for both forms are different from 3, the value expected for poled films in which the chromophores have a one dimensional first hyperpolarizability tensor,[24] indicating that there is not only a charge transfer along the direction of the dipole moment.[20g,25,26]

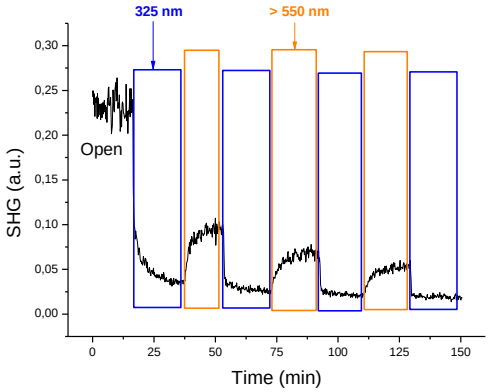

Figure 9. SHG Photoswitch of the **PtDTE1/**PS film starting from the open form.

These results prompted us to investigate, after poling, the SHG photoswitching of polystyrene films based on **PtDTE1** starting from the open form (Figure 9) with the fundamental and SH beams p-polarized. It turns out that the intensity of the SHG signal decreases after UV irradiation, as the closed form is generated. Once a stable plateau is reached, when the UV irradiation is stopped and the visible light (λ>550nm) turned on, the SHG intensity increases as the closed form converts back to the open form. As expected, exposure to visible light of a freshly prepared poled polystyrene film based on the closed form of **PtDTE1** leads to an increase of the SHG intensity, due to the ring-opening of DTE (Figure S25).

The loss of some SHG intensity during the sequential on/off processes (Figures 9 and S25) is due to the irreversible loss of orientation through the photoisomerization processes. In the future, stability improvement could be reasonably achieved by using the cross-linking technique for the preparation of the polymer films.

It is interesting to point out that the polymer film based on **PtDTE1(o)** shows a higher SHG intensity than the related closed form whereas the closed form is more NLO-active in solution according to EFISH measurements. This difference between the macroscopic and the molecular behavior, which has been previously reported for organic compounds based on phenyl-substituted dithienylethene,[20g] confirms the importance of the geometry and charge transfers inside the chromophores on the macroscopic NLO response.

Theoretical calculations. We also performed a theoretical analysis to give a complementary light on the investigated systems. The methods used are detailed in the experimental section and follow previous successful Time-Dependent Density

Functional Theory (TD-DFT) studies of organic and metal-containing DTE switches.[6,27] The DFT-obtained geometries are similar to the one of similar systems.[6,27] Nevertheless, let us note that (i) the angle between the thienyl ring of the DTE unit and the phenyl ring attains 23° for **PtDTE1(o)** but 0° for **PtDTE1(c)**, indicating that the increase of planarity between the two moieties when going from the open to the closed DTE found in the XRD structure is not purely related to a packing effect; and (ii) the central CC bond in the closed form is 1.54 Å long, which is typical of closed DTE units. More importantly, in **PtDTE2**, the linker provides some conformational flexibility and several minimal structures could be obtained with DFT. As the obtained electronic spectra of these conformers are similar to the one of the most stable structures, we report below the results obtained on the conformer presenting the lowest free energy only.

For **Pt1**, TD-DFT returns two dipole-allowed singlet states below 400 nm: 426 nm (*f*=0.12) and 419 nm (*f*=0.03), which correspond to the main absorption band shown in the inset of Figure 4a. These two transitions respectively present strongly dominating HOMO-LUMO and HOMO-LUMO+1 characters. As can be seen in Figure 10, the HOMO is localized on the thiophene, phenyl, Pt and Cl atoms, whereas the LUMO and LUMO+1 are centered on the (N^C^N) fragment. Therefore these transitions have a significant CT character. In **PtDTE1(o)**, the corresponding transitions are located at 417 nm (*f*=0.11) and 409 nm (*f*=0.03), blueshifted by ca. 10 nm compared to **Pt1**. These transitions have the same character as in **Pt1** and the associated MOs present the same shape (Figure 10). In **PtDTE2(o)**, the main absorption band at 418 nm (*f*=0.17) corresponds to a HOMO-LUMO transition, clearly purely localized on the (N^C^N)PtCl moiety. In the closed forms, **PtDTE1(c)** and **PtDTE2(c)**, a new excited-state appears at 597 nm (*f*=0.54) and 587 nm (*f*=0.44). These states are ascribed to a HOMO-LUMO transition mainly localized on the DTE core, as expected. The delocalization of the HOMO and LUMO on the (N^C^N) fragment is indeed present but limited even in the case of **PtDTE1(c)** (Figure S26). In **PtDTE2(c)**, the absorption band characteristic of the (N^C^N) fragment is computed at 419 nm, and is therefore almost unperturbed by the ring-closure of the DTE, which is both a logical consequence of the used linker and, is also consistent with experiment. The situation is different in **PtDTE1(c)**: TD-DFT predicts a weak absorption at 467 nm (*f*=0.03) and a strong absorption at 399 nm (*f*=0.28), that were not present in **PtDTE1(o)**. These vertical transitions correspond to a HOMO to LUMO+1 and a HOMO-1 to LUMO electronic promotions, respectively. As can be concluded from Figure S27, the first weak band implies a significant CT character from the DTE towards the (N^C^N) fragment, whereas the second one involves a CT in the reverse direction.

Obviously, the virtual orbitals displayed in Figure 10 are localized on the (N^C^N) moiety so that electronic promotion to these orbitals will not trigger a direct photocylization. Indeed, it was shown that the open to closed transformation in DTE needs to go through a so-called *photochromic orbital*.[28] Clearly in both **PtDTE1(o)** and **PtDTE2(o)**, this orbital is the LUMO+2 that presents a bonding character for the to-be-formed C-C bond as well as a large contribution on the two reactive carbon atoms (Figure S28).

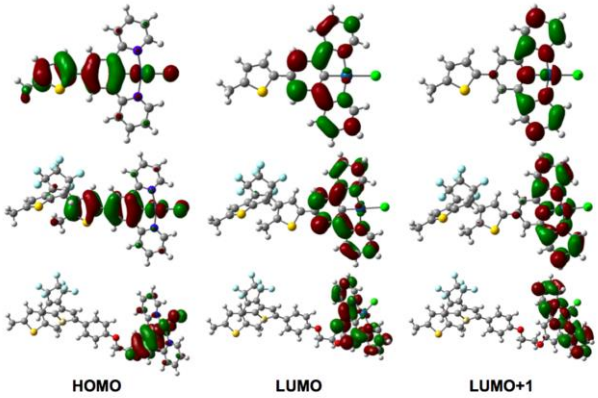

Figure 10. Molecular orbitals for the different systems (threshold used: 0.03 au). From top to bottom: **Pt1**, **PtDTE1(o)** and **PtDTE2(o)**.

In the former compound, it is also noticeable that no significant impact of the directly linked organometallic moiety is noticed, so that one does expect the photochromism of the DTE to be perturbed. This *photochromic orbital* can be accessed by a dipole-allowed transition located by TD-DFT at 364 nm (*f*=0.04) and 363 nm (*f*=0.05) for **PtDTE1(o)** and **PtDTE2(o)**, respectively. This is consistent with the fact that irradiation at 350 nm induces an efficient and alike photoswitching process in both compounds. However, irradiation at 450 nm also triggers the photochromic reaction, though on a slower rate, especially in **PtDTE2(o)** (Figure S19). In that case the topology of the virtual MOs seems unsuited (Figure 10). For **PtDTE1(o)** the 450 nm absorption likely induces photochromism after intersystem crossing to the lowest triplet excited-state. Indeed, the topology of the spin density for this state (optimal triplet geometry, Figure S29 in the ESI), displays a significant contribution on one of the two reactive carbon atoms, which is enough to induce the photochromic reaction.[28] In contrast, in **PtDTE2(o)**, the observed results is likely related to a through-space energy transfer between the two moieties.

Conclusions

In summary, two new photochromic cyclometalated (N^C^N) platinum(II) complexes have been designed and synthetized with a DTE unit connected on the *para*-position of the (N^C^N) cyclometalated ligand, directly (**PtDTE1**) or through an insulator and flexible link (**PtDTE2**). Both complexes have demonstrated excellent photochromic behavior upon UV or visible light irradiation. The first X-ray diffraction studies on both open and close isomers of a DTE-based cyclometalated Pt(II) complex (**PtDTE1**) have been herein presented. In particular, the unexpectedly good photoisomerization of **PtDTE2** upon visible light excitation has been rationalized, by means of joint experimental and theoretical investigations, as intramolecular energy transfer between the (N^C^N)PtCl and DTE parts which are bring closer thanks to the flexible linkage. This efficient photochromism for **PtDTE1** and **PtDTE2** leads to a significant NLO photo-modulation, both in solution and in thin films, of particular interest for the design of reversible NLO switches for emerging photonic technologies. In addition, the photo-regulation of the luminescence has been demonstrated for both complexes reported here.

Experimental Section

Synthesis: The synthesis and characterization of all ligands and complexes is reported in the Supporting Information.

Absorption and emission measurements.

UV/vis absorption spectra were recorded with a Specord 205 UV-Vis-NIR spectrophotometer using quartz cuvettes of 1 cm pathlength. Changes in absorption upon continuous light irradiation were recorded every 500 seconds with 60 seconds of integration time, on CH_2Cl_2 solution at DO = 0.1 at the excitation wavelength (350 or 450 nm). Light excitation was applied with a Thorlabs lamp SLS201L equipped with the appropriate single wavelength light filter (350FS 10-25 or 450FS 40-25).

Photoisomerization experiments in solution have been made using a LS series Light Source of ABET technologies, Inc (150 W xenon lamp), with single wavelength light filters "350FS 10-25" or "450FS 40-25" for ring-closure and "580FS 10-25" for cycloreversion. Irradiations for ^{1}H NMR experiment have been made using a Rayonet® with 350 nm light emitting lamps (213 μW cm^{-2}).

Steady-state luminescence spectra were measured using an Edinburgh FS920 Steady State Fluorimeter combined with a FL920 Fluorescence Lifetime Spectrometer. The spectra were corrected for the wavelength dependence of the detector, and the quoted emission maxima refer to the values after correction. Luminescence quantum yields were determined using $[Ru(bpy)_3]Cl_2$ (Φ = 0.028 in air-equilibrated aqueous solution)[29] as standard and correcting for the refractive index. Life-times measurements were conducted with 440 nm diode laser excitation (EPL-series). Variable temperature emission measurements were preformed using the cryostat Optistat DN (Oxford Instruments).

Second order nonlinear optical measurements:

EFISH measurements. All EFISH measurements[11] were carried out at the Dipartimento di Chimica of the Università degli Studi di Milano, in CH_2Cl_2 solutions at a concentration of 5-8 x 10^{-4} M, working with a non-resonant incident wavelength of 1.907 μm, obtained by Raman-shifting the fundamental 1.064 μm wavelength produced by a Q-switched, mode-locked Nd^{3+}:YAG laser manufactured by Atalaser. The apparatus for the EFISH measurements is a prototype made by SOPRA (France). The reported $\mu\beta_{EFISH}$ values are the mean values of 16 successive measurements performed on the same sample. The sign of μβ is determined by comparison with the reference solvent (DMF or CH_2Cl_2).

Preparation of composite films and SHG measurements Thin films of the complex PtDTE1 in open form (5% w/w relative to the polymer) dispersed in poly(methyl methacrylate) (PMMA) or polystyrene (PS) were prepared by spin-coating a few drops of a dichloromethane solution on ordinary non-pretreated glass substrates (thickness 1 mm) previously cleaned with water/acetone. The spinning parameters were set at the following values: RPM 1 = 800; ramp 1 = 1 s, time 1 = 5 s; RPM 2 = 2000; ramp 2 = 4 s, time 2 = 83 s. Closed form of the PtDTE1 film in PS or PMMA matrix was obtained from PtDTE1 in open form after irradiation with UV light at 325 nm (continuous wave (cw) mode power, 15mW) for 15 minutes. The thickness of the films: 1.83 ± 0.11μm for PS and 0.96 ± 0.06μm for PMMA matrix were measured using an α-step stylus profilometer DektaK XT. Electronic absorption spectra of the composite films were recorded by a spectrophotometer Mahamatzu 3600.

Corona Poling Setup. The fundamental incident light was generated by a 1064 nm Q-switched Nd:YAG laser. The output pulse was attenuated to 0.5 mJ and was focused on the sample, placed over the hot stage. Moreover, the fundamental beam was polarized in the incidence plane (p-polarized) with an incidence angle of about 55° respect to the sample in order to optimize the SHG signal. Poling process was performed in a N_2 atmosphere and a corona-wire voltage (up to 10 kV across a 10 mm gap) was applied. After rejection of the fundamental beam by an interference filter and a glass cutoff filter, the p-polarized SHG signal at 532 nm was detected with a UV-vis photomultiplier (PT). The output signal from the PT was set to a digital store oscilloscope and then processed by a computer with dedicated software.

Maker Fringe and Second Harmonic Photoswitch. In the Maker fringe experiment, the second harmonic (SH) intensity was detected as a function of the incidence angle of the fundamental beam and normalized with respect to that of a calibrated quartz crystal wafer (X-cut) 1 mm thick whose d_{11} is 0.46 pm/V. The incidence angle was changed by rotating the poled film, while the polarization of the fundamental and SH beam could be changed by a half-wave plate and a cube beam splitter, respectively. In order to determine the nonzero independent components of the susceptibility tensor for poled films ($C_{\infty v}$ symmetry) Maker fringe measurements were conducted with different polarizations: p → p, s → p, and 45 → s. In the SHG photoswitch experiment, the poled film was rotated at incidence angle of 55° and the fundamental and SH beams were p-polarized. With the purpose of changing the photocyclization state, the poled film was alternately irradiated with UV light at 325 nm (continuous wave (cw) mode power, 15mW) and visible light with a cutoff filter at 550 nm (cw mode power, 140 mW).

Computational details:

All simulations have been achieved with the Gaussian09 program,[30] using Density Functional Theory (DFT) and Time-Dependent DFT (TD-DFT), for the ground and excited state properties, respectively. The computational protocol proceeds through several steps. (i) The optimal ground-state geometrical parameters have been determined with the PBE0 functional[31] completed with the so-called D3-BJ model[32] to describe dispersion interactions. These calculations use the LanL2DZ pseudo-potentials and basis set for all atoms completed with additional orbitals.[33] Spherical *d* (5D) and *f* (7F) functions were applied. These calculations were performed in solution using the PCM model.[34] (ii) The vibrational spectrum of each derivative has been determined analytically at the same level of theory as in the first step and it has been checked that all structures correspond to true minima of the potential energy surface. (iii) TD-DFT calculations, using the same level of theory as in steps 1 and 2 (PBE0/LanL2DZ+additional functions), were performed to model the excited-states. 40 excited-states were typically determined. These calculations use the PCM model, in its linear-response approach applying the *non-equilibrium* regime, to account for solvation effects. (iv) The dipole moments used in the NLO study were determined analytically. These calculations have been performed with the range-separated hybrid ωB97X-D functional,[35] using the same basis set as above and considering solvent effects during the calculations.

Associated Content

^{1}H, ^{19}F and ^{13}C NMR data and spectra, elemental analysis, crystallographic data, additional emission spectra, NLO data (poling studies, SHG measurements), theoretical data (frontier MOs and spin density differences).

Acknowledgements ((optional))

We thank CNRS (PICS Rennes-Milan) and the National Interuniversity Consortium of Materials Science and Technology (Project INSTMMI012) for financial support and l'Università Italo Francese (Progetto Galileo 2015/2016; G15_50) for mobility support. Regione Lombardia and Fondazione Cariplo are acknowledged for the use of instrumentation purchased through the SmartMatLab Centre project (2014). This work used computational resources of the CCIPL installed in Nantes and of the CINES/IDRIS

Keywords: photochromism • second-order nonlinear optics • luminescence • cyclometalated platinum complexes • dithienylethene

[1] E. C. Harvey, E. C., Feringa, B. L., Vos, J. G., Browne, W. R., Pryce, M. T. Transition metal functionalized photo- and redox-switchable diarylethene based molecular switches. *Coord. Chem. Rev*., **2015**, *282*, 77-86.

[2] a) Pizzotti, M., Ugo, R., Roberto, D., Bruni, S., Fantucci, P., Rovizzi, C. Organometallic Counterparts of Push−Pull Aromatic Chromophores for Nonlinear Optics: Push−Pull Heteronuclear Bimetallic Complexes with Pyrazine and *trans*-1,2-Bis(4-pyridyl)ethylene as Linkers. *Organometallics*, **2002**, *21*, 5830-5840. b) Valore, A., Colombo, A., Dragonetti, C., Righetto, S., Roberto, D., Ugo, R., De Angelis, F., Fantacci, S. Luminescent cyclometallated Ir(III) and Pt(II) complexes with β-diketonate ligands as highly active second-order NLO chromophores. *Chem. Commun*., **2010**, *46*, 2414-2416. c) Valore, A., Cariati, E., Dragonetti, C., Righetto, S., Roberto, D., Ugo, R., De Angelis, F., Fantacci, S., Sgamellotti, A., Macchioni, A., Zuccaccia, D. Cyclometalated Ir^{III} Complexes with Substituted 1,10-Phenanthrolines: A New Class of Efficient Cationic Organometallic Second-Order NLO Chromophores. *Chem. Eur. J.,* **2010**, *16,* 4814-4825.

[3] a) Irie, M. Diarylethenes for Memories and Switches. *Chem. Rev*., **2000**, *100*, 1685-1716. b) Irie, M., Fukaminato, T., Matsuda, M., Kobatake, S. Photochromism of Diarylethene Molecules and Crystals: Memories, Switches, and Actuators. *Chem. Rev*., **2014**, *114*, 12174-12277.

[4] a) Bleger, D., Hecht, S. Visible-Light-Activated Molecular Switches. *Angew. Chem. Int. Ed.,* **2015**, *54*, 11338-11349. b) Babii, O., Afonin, S., Garmanchuk, L. V., Nikulina, V. V., Nikolaienko, T. V., Storozhuk, O. V., Shelest, D. V., Dasyukevich, O. I., Ostapchenko, L. I., Iurchenko, V., Zozulya, S., Ulrich, A. S., Komarov, I. V. Direct Photocontrol of Peptidomimetics: An Alternative to Oxygen-Dependent Photodynamic Cancer Therapy. *Angew. Chem. Int. Ed*., **2016**, *55*, 5493-5496. c) Mosciatti, T., del Rosso, M. G., Herder, M., Frisch, J., Koch, N., Hecht, S., Orgiu, E., Samorì, P. Light-Modulation of the Charge Injection in a Polymer Thin-Film Transistor by Functionalizing the Electrodes with Bistable Photochromic Self-Assembled Monolayers. *Adv. Mater.,* **2016**, *28*, 6606-6611. d) Jia, C., Migliore, A., Xin, N., Huang, S., Wang, J., Yang, Q., Wang, S., Chen, H., Wang, D., Feng, B., Liu, Z., Zhang, G., Qu, D.-H., Tian, H., Ratner, M. A., Xu, H. Q., Nitzan, A., Guo, X. Covalently bonded single-molecule junctions with stable and reversible photoswitched conductivity. *Science,* **2016**, 352, 1443-1445.

[5] a) Guerchais, V., Ordronneau, L., Le Bozec. H. Recent developments in the field of metal complexes containing photochromic ligands: Modulation of linear and nonlinear optical properties *Coord. Chem. Rev.*, **2010**, *254*, 2533-2545. b) Hasegawa, Y., Nakagawa, T., Kawai, T. Recent progress of luminescent metal complexes with photochromic units. *Coord. Chem. Rev*., **2010**, *254*, 2643-2651. c) Di Bella, S., Dragonetti, C., Pizzotti, M., Roberto, D., Tessore, F., Ugo, R. *in Topics in Organometallic Chemistry 28. Molecular Organometallic Materials for Optics*, Vol. 28 (Eds: H. Le Bozec, V. Guerchais), Springer, **2010**, 1. d) Xue, X., Wang, H., Han, Y., Hou, H. Photoswitchable nonlinear optical properties of metal complexes. *Dalton Trans.*, **2018**, *47*, 13-22. e) Ko, C.-C., Yam, V. W.-W. Coordination Compounds with Photochromic Ligands: Ready Tunability and Visible Light-Sensitized Photochromism. *Acc. Chem. Res*. **2018**, *51*, 149-159.

[6] a) Boixel, J., Guerchais, V., Le Bozec, H., Jacquemin, D., Amar, A., Boucekkine, A., Colombo, A., Dragonetti, C., Marinotto, D., Roberto, D., Righetto, S., De Angelis, R. Second-Order NLO Switches from Molecules to Polymer Films Based on Photochromic Cyclometalated Platinum(II) Complexes. *J. Am. Chem. Soc*., **2014**, *136*, 5367-5375. b) Boixel, J., Guerchais, V., Le Bozec, H., Chantzis, A., Jacquemin, D., Colombo, A., Dragonetti, C., Marinotto, D., Roberto, D. Sequential double second-order nonlinear optical switch by an acido-triggered photochromic cyclometallated platinum(II) complex. *Chem. Commun.*, **2015**, *51*, 7805-7808. c) Boixel, J., Zhu, Y., Le Bozec, H., Benmensour, M. A., Boucekkine, A., Wong, K. M.-C., Colombo, A., Roberto, D., Guerchais, V., Jacquemin, D. Contrasted photochromic and luminescent properties in dinuclear Pt(II) complexes linked through a central dithienylethene unit. *Chem. Commun*., **2016**, *52*, 9833-9836.

[7] a) Rossi, E., Colombo, A., Dragonetti, C., Righetto, S., Roberto, D., Ugo, R., Valore, A., Williams, J. A. G., Grazia Lobello, M., De Angelis, F., Fantacci, S., Ledoux-Rak, I., Singh, A., Zyss, J. Tuning the Dipolar Second-Order Nonlinear Optical Properties of Cyclometalated Platinum(II) Complexes with Tridentate N^C^N Binding Ligands. *Chem. Eur. J.,* **2013**, *19*, 9875-9883. b) Nisic, F., Cariati, E., Colombo, A., Dragonetti, A., Fantacci, S., Garoni, E., Lucenti, E., Righetto, S., Roberto, D., Williams, J. A. G. Tuning the dipolar second-order nonlinear optical properties of 5-π-delocalized-donor-1,3-di(2-pyridyl)benzenes, related cyclometallated platinum(II) complexes and methylated salts. *Dalton Trans*., **2017**, *46*, 1179-1185. c) Baggi, N., Garoni, E., Colombo, A., Dragonetti, C., Righetto, S., Roberto, D., Boixel, J., Guerchais, V., Fantacci, S. Design of cyclometallated 5-π-delocalized donor-1,3-di(2-pyridyl)benzene platinum(II) complexes with second-order nonlinear optical properties. *Polyhedron*, **2018**, *140*, 74-77.

[8] a) Williams, J. A. G., Beeby, A., Davies, E. S., Weinstein, J. A., Wilson, C. An Alternative Route to Highly Luminescent Platinum(II) Complexes: Cyclometalation with N^C^N-Coordinating Dipyridylbenzene Ligands. *Inorg. Chem.,* **2003**, *42*, 8609-8611. b) Farley, S. J., Rochester, D. L., Thompson, A. L., Howard, J. A. K., Williams, J. A. G. Controlling Emission Energy, Self-Quenching, and Excimer Formation in Highly Luminescent N^C^N-Coordinated Platinum(II) Complexes. *Inorg. Chem*., **2005**, *44*, 9690-9703. c) Develay, S., Williams, J. A. G. Intramolecular excimers based on rigidly-linked platinum(II) complexes: intense deep-red triplet luminescence in solution. *Dalton. Trans*., **2008**, 4562-4564. d) Rochester, D. L., Develay, S., Zalis, S., Williams, J. A. G. Localised to intraligand charge-transfer states in cyclometalated platinum complexes: an experimental and theoretical study into the influence of electron-rich pendants and modulation of excited states by ion binding. *Dalton Trans.*, **2009**, 1728-1741. e) Wang, Z., Turner, E., Mahoney, V., Madakuni, S., Groy, T., Li, J. Facile Synthesis and Characterization of Phosphorescent Pt(N^C^N)X Complexes. *Inorg. Chem*., **2010**, *49*, 11276-11286. f) Freeman, G. R., Williams, J. A. G. *Top. Organomet. Chem*., **2013**, *40*, 89-130.

[9] a) Cocchi, M., Virgili, D., Fattori, V., Rochester, D. L., Williams, J. A. G. N^C^N-Coordinated Platinum(II) Complexes as Phosphorescent Emitters in High-Performance Organic Light-Emitting Devices. *Adv. Funct. Mater.,* **2007**, *17*, 285-289. b) Rossi, E., Colombo, A., Dragonetti, C., Roberto, D., Demartin, D., Cocchi, M., Brulatti, P., Fattori, V., Williams, J. A. G. From red to near infra-red OLEDs: the remarkable effect of changing from X = –Cl to –NCS in a cyclometallated [Pt(N^C^N)X] complex {N^C^N = 5-mesityl-1,3-di-(2-pyridyl)benzene}. *Chem. Commun.,* **2012**, *48,* 3182-3184. c) Rossi, E., Colombo, A., Dragonetti, C., Roberto, D., Ugo, R., Valore, A., Falciola, L., Brulatti, P., Cocchi, P., Williams, J. A. G. Novel N^C^N-cyclometallated platinum complexes with acetylide co-ligands as efficient phosphors for OLEDs. *J. Mater. Chem.,* **2012**, *22*, 10650-10655. d) Tang, M.-C., Chan, A. K.-W., Chan, M.-Y., Yam, V. W.-W. *Top. Curr. Chem.*, **2016**, 374:46. e) Chan, A. K.-W., Ng, M., Wong, Y.-C., Chan, M.-Y., Wong, W.-T., Yam, V. W.-W. Synthesis and Characterization of Luminescent Cyclometalated Platinum(II) Complexes with Tunable Emissive Colors and Studies of Their Application in Organic Memories and Organic Light-Emitting Devices. *J. Am. Chem. Soc.,* **2017**, *139*, 10750-10761.

[10] Baggaley, E., Botchway, S. W., Haycock, J. W., Morris, H., Sazanovich, I. V., Williams, J. A. G., Weinstein, J. A. Long-lived metal complexes open up microsecond lifetime imaging microscopy under multiphoton excitation: from FLIM to PLIM and beyond. *Chem. Sci*., **2014**, *5*, 879-886.

[11] a) Levine, B. F., Bethea, C. G. Molecular hyperpolarizabilities determined from conjugated and nonconjugated organic liquids. *Appl. Phys. Lett.,* **1974**, *24*, 445-447. b) Levine, B.F., Bethea, C.G. Second and third order hyperpolarizabilities of organic molecules. *J. Chem. Phys.* **1975**, *63*, 2666-2682. c) Ledoux, I., Zyss, J. Influence of the molecular environment in solution measurements of the Second-order optical susceptibility for urea and derivatives. *J. Chem. Phys.,* **1982**, *73*, 203-213.

[12] a) Myles, A. J., Wigglesworth, T. J., Branda, N. R. A Multi-Addressable Photochromic 1,2-Dithienylcyclopentene-Phenoxynaphthacenequinone Hybrid. *Adv. Mater*., **2003**, *15*, 745-748. b) Pu, S., Jiang, D., Liu, W., Liu, G., Cui, S. Multi-addressable molecular switches based on photochromic diarylethenes bearing a rhodamine unit. *J. Mater. Chem*., **2012**, *22*, 3517-3526. c) Pu, S., Liu, W., Miao, W. Photochromism of new unsymmetrical isomeric diarylethenes bearing a methoxyl group. *J. Phys. Org. Chem.,* **2009**, *22*, 954-963.

[13] Colombo, A., Fiorini, F., Septiadi, D., Dragonetti, C., Nisic, F., Valore, A., Roberto, D., Mauro, M., De Cola, L.. Neutral N^C^N terdentate luminescent Pt(II) complexes: their synthesis, photophysical properties, and bio-imaging applications. *Dalton Trans*., **2015**, *44*, 8478-8487.

[14] a) Kobatake, S., Yamada, M., Yamada, T., Irie, M. Photochromism of 1,2-Bis(2,5-dimethyl-3-thienyl)perfluoro- cyclopentene in a Single Crystalline Phase. *J. Am. Chem. Soc.,* **1999**, *121,* 8450-8456. b) Kobatake, S., Shibata,

K., Uchida, K., Irie, M. Photochromism of 1,2-Bis(2-ethyl-5-phenyl-3-thienyl)perfluorocyclopentene in a Single-Crystalline Phase. Conrotatory Thermal Cycloreversion of the Closed-Ring Isomer. *J. Am. Chem. Soc.,* **2000**, *122,* 12135-12141. c) Irie, M., Kobatake, S., Horichi, M. Reversible surface morphology changes of a photochromic diarylethene single crystal by photoirradiation. *Science,* **2001**, *291*, 1769-1772. d) Higashiguchi, K., Matsuda, K., Matsuo, M., Yamada, T., Irie, M. Photochromic reactivity of a dithienylethene dimer *J. Photochem. Photobiol. A: Chemistry,* **2002***, 152,* 141-146. e) Yamaguchi, T., Fujita, Y., Irie, M. Photochromism of a novel 6π conjugate system having a bis(2,3′-benzothienyl) unit. *Chem. Commun.,* **2004**, 1010-1011. f) Morimoto, M., Irie, M. A Diarylethene Cocrystal that Converts Light into Mechanical Work. *J. Am. Chem. Soc*., **2010**, *132*, 14172-14178. g) Motoyama, K., Li, H., Koike, T., Hatakeyama, M., Yokojima, S., Nakamura, S., Akita, M. Photo- and electro-chromic organometallics with dithienylethene (DTE) linker, L2CpM-DTE-MCpL2: Dually stimuli-responsive molecular switch. *Dalton Trans*., **2011**, *40*, 10643-1065. h) Ohshima, S. Morimoto, M., Irie, M. Light-driven bending of diarylethene mixed crystals. *Chem. Sci.*, **2015**, *6*, 5746-5752.

[15] Brayshaw, S. K., Schiffers, S., Stevenson, A. J., Teat, S. J., Warren, M. R., Bennett, R. D., Sazanovich, I. V., Buckley, A. R., Weinstein, J. A., Raithby, P. R. Highly Efficient Visible-Light Driven Photochromism: Developments towards a Solid-State Molecular Switch Operating through a Triplet- Sensitised Pathway. *Chem. Eur. J*., **2011**, *17*, 4385-4395.

[16] a) For an example of the effect of the coordination of Zinc ion on DTE-based bipyridine ligands on the ring- closure/opening processes, see: Ordronneau, L., Aubert, V., Métivier, R., Ishow, E., Boixel, J., Nakatani, K., Ibersiene, F., Hammoutène, F., Boucekkine, A., Le Bozec, H., Guerchais, V. Tunable double photochromism of a family of bis-DTE bipyridine ligands and their dipolar Zn complexes. *Phys. Chem. Chem. Phys.,* **2012**, *14*, 2599-2605. b) Roberts, M. N., Nagle, J. K., Finden, J. G., Branda, N. R., Wolf, M. O. Linker-Dependent Metal-Sensitized Photoswitching of Dithienylethenes**.** *Inorg. Chem*., **2009**, *48*, 19-21. c) Roberts, M. N., Nagle, J. K., Majewski, M. B., Finden, N., Branda, N. R., Wolf, M. O. Charge Transfer and Intraligand Excited State Interactions in Platinum-Sensitized Dithienylethenes. *Inorg. Chem.*, **2011**, *50*, 4956-496.

[17] a) Fernandez-Acebes, A., Lehn, J.-M. Optical Switching and Fluorescence Modulation Properties of Photochromic Metal Complexes Derived from Dithienylethene Ligands. *Chem. Eur. J.*, **1999**, *5*, 3285-3292. b) Lee, P. H.-M., Ko, C.-C., Zhu, O., Yam, V. W.-W. Metal Coordination-Assisted Near-Infrared Photochromic Behavior: A Large Perturbation on Absorption Wavelength Properties of N,N-Donor Ligands Containing Diarylethene Derivatives by Coordination to the Rhenium(I) Metal Center. *J. Am. Chem. Soc*., **2007**, *129*, 6058-6059. c) Ordronneau, L., Aubert, V., Metivier, R., Ishow, E., Boixel, J., Nakatani, K., Ibersiene, F., Hammoutene, D., Boucekkine, A., Le Bozec, H., Guerchais, V. Tunable Stepwise Photochromism of a Family of Bis-DTE Bipyridine Ligands and their Dipolar Zn Complexes. *Phys. Chem. Chem. Phys.,* **2012**, *14*, 2599-2605.

[18] Yam, V. W.-W., Chan, K. H.-Y., Wong, K. M.-C. Chu, B. W.-K. Luminescent Dinuclear Platinum(II) Terpyridine Complexes with a Flexible Bridge and "Sticky Ends". *Angew. Chem. Int. Ed.,* **2006**, *45*, 6169-6173.

[19] a) Dulic, D., Kudernac, T., Puzys, A., Feringa, B. L., van Wees, B. J. Temperature Gating of the Ring-Opening Process in Diarylethene Molecular Switches. *Adv. Mater*., **2007**, *19*, 2898-2902. b) Kudernac, T., Kobayashi, T., Uyama, A., Uchida, K., Nakamura, S., Feringa, B. L. Tuning the Temperature Dependence for Switching in Dithienylethene Photochromic Switches. *J. Phys. Chem. A*, **2013**, *117*, 8222-8229. c) Cox, J. M., Walton, I. M., Patel, D. G., Xu, M., Chen, Y.-S., Benedict, J. B. The Temperature Dependent Photoswitching of a Classic Diarylethene Monitored by *in Situ* X-ray Diffraction. *J. Phys. Chem. A*, **2015**, *119*, 884-888.

[20] a) Loucif-Saibi, R., Nakatani, K., Delaire, J. A., Dumont, M., Sekkat, Z. Photoisomerization and second harmonic generation in disperse red one-doped and -functionalized poly(methyl methacrylate) films. *Chem. Mater.,* **1993**, *5*, 229-236. b) Atassi, Y., Dalaire, J. A., Nakatani, K. Coupling between Photochromism and Second-Harmonic Generation in Spiropyran- and Spirooxazine-Doped Polymer Films. *J. Phys. Chem.,* **1995**, *99*, 16320-16326. c) Rodriguez, F. J., Sanchez, V C., Villacampa, B., Alcalà, R., Cases, R., Millaruelo, M., Oriol, L. Optical anisotropy and non-linear optical properties of azobenzene methacrylic polymers. *Polymer,* **2004**, *45*, 2341-2348. d) Nakatani, K., Delaire, J. A. Reversible Photoswitching of Second-Order Nonlinear Optical Properties in an Organic Photochromic Crystal. *Chem. Mater.,* **1997**, *9*, 2682-2684. e) Wang, C. H., Gu, S. H., Guan, H. W. Polar order and relaxation of second order nonlinear optical susceptibility in an electric field polarized amorphous polymer. *J. Chem. Phys.,* **1993**, *99,* 5597-5604. f) Atassi, Y., Chauvin, J., Delaire, J. A., Delouis, J. F., Fanton-Maltey, I., Nakatani, K. Photoinduced manipulations of photochromes in polymers: Anisotropy, modulation of the NLO properties and creation of surface gratings. *Pure Appl. Chem.,* **1998**, *70*, 2157-2166. g) Marinotto, D., Castagna, R., Righetto, R., Dragonetti, C., Colombo, A., Bertarelli, C., Garbugli, M., Lanzani, G. Photoswitching of the Second Harmonic Generation from Poled Phenyl-Substituted Dithienylethene Thin Films and EFISH Measurements. *J. Phys. Chem. C,* **2011**, *115*, 20425-20432.

[21] Andrews, R. D., Hammack, T. J., *J. Polym. Sci., Part B*, **1965**, *3*, 655-657.

[22] a) Page, R. H., Jurich, M. C.,Beck, B., Sen, A., Twieg, R. J., Swalen, J. D., Bjorklund, G. C., Wilson, C. G. Electrochromic and optical waveguide studies of corona-poled electro-optic polymer films. *J. Opt. Soc. Am. B,* **1990**, *7*, 1239-1250. b) Mortazavi, M. A., Knoesen, A., Kowel, S. T., Higgins, B. G., Dienes, A. Second-harmonic generation and absorption studies of polymer–dye films oriented by corona-onset poling at elevated temperatures. *J. Opt. Soc. Am. B,* **1989**, *6*, 733-741.

[23] Herman, W. N., Hayden, L. M. Maker fringes revisited: second-harmonic generation from birefringent or absorbing materials. *J. Opt. Soc. Am. B,* **1995**, *12,* 416-427.

[24] Prasad, P. N., Williams, D. *Introduction to Nonlinear Optical Effects in Molecules and Polymers*; Wiley: New York, **1991**. b) Burland, D. M., Miller, R. D., Walsh, C. Second-order nonlinearity in poled-polymer systems. *Chem. Rev.,* **1994**, *94*, 31-75. c) Ghebremichael, F., Kuzyk, M. G., Lackritz, H. S. Nonlinear optics and polymer physics. *Prog. Polym. Sci.,* **1997**, *22,* 1147-1201.

[25] a) Rojo, G., Agullò-Lòpez, F., Del Rey, B., Torres, T. Macroscopic and microscopic second-harmonic response from subphthalocyanine thin films. *J. Appl. Phys.,* **1998**, *84*, 6507-6512. b) Di Bella, S., Fragalà, I. *New J. Chem.* **2002**, *26*, 285-290.

[26] Kielich, S. Optical second-harmonic generation by electrically polarized isotropic media. *IEEE J. Quantum Electron.,* **1969**, *5*, 562-568.

[27] a) Chen, K. J., Laurent, A. D., Jacquemin, D. Strategies for Designing Diarylethenes as Efficient Nonlinear Optical Switches. *J. Phys. Chem. C*, **2014**, *118*, 4334-4345.

[28] a) Perrier, A., Maurel, F., Jacquemin, D. Single Molecule Multiphotochromism with Diarylethenes. *Acc. Chem. Res.*, **2012**, *45*, 1173-1182. b) Perrier, A., Maurel, F., Jacquemin, D. Interplay Between Electronic and Steric Effects in Multiphotochromic Diarylethenes. *J. Phys. Chem. C*, **2011**, *115*, 9193-9203.

[29] Demas, J. N., Crosby, G. A. Measurement of photoluminescence quantum yields. Review. *J. Phys. Chem.*, **1971**, *75*, 991-1024.

[30] Frisch, M. J. Gaussian 09 Revision D.01, **2009**, Gaussian Inc. Wallingford CT. **2009**.

[31] Adamo, C., Barone, V. Toward reliable density functional methods without adjustable parameters: The PBE0 model. *J. Chem. Phys.,* **1999**, *110*, 6158-6170.

[32] Grimme, S., Ehrlich, S., Goerigk, L. Effect of the damping function in dispersion corrected density functional theory. *J. Comp. Chem*., **2011**, *32*, 1456-1465.

[33] The additional atomic orbitals are: on C: *d* with □= 0.587; on N : *d* with □= 0.736; on F: *d* with □= 1.577; on S: *d* with □= 0.496; on Cl: *d* with □= 0.648; on Pt: *f* with □= 0.802.

[34] Tomasi, J., Mennucci, B., Cammi, R. Quantum Mechanical Continuum Solvation Models. *Chem. Rev.,* **2005**, *105*, 2999-3094.

[35] Chai, J. D., Head-Gordon, M. Long-range corrected hybrid density functionals with damped atom-atom dispersion corrections. *Phys. Chem. Chem. Phys.,* **2008**, *10*, 6615-6170.

The Table of Contents

Photochromic DTE-Substituted -1,3-di(2-pyridyl)benzene Platinum(II) Complexes: Photo-modulation of Luminescence and Second-order Nonlinear Optical Properties

Hong Zhao, Eleonora Garoni, Thierry Roisnel, Alessia Colombo, Claudia Dragonetti, Daniele Marinotto, Stefania Righetto, Dominique Roberto, Denis Jacquemin*, Julien Boixel*, Véronique Guerchais*[a]

Synopsis

DTE-substituted-1,3-di(2-pyridyl)benzene (N^C^N)platinum(II) complexes display excellent photochromic properties upon UV or visible irradiation, irrespective of the connecting mode between the DTE unit and the platinum(II) moiety. The efficient photoisomerization/cycloreversion processes lead to a significant NLO photo-modulation, both in solution and in thin films. In addition, the emission can be photo-controlled.